Probing the magnetic order in $(Cr_{84}Re_{16})_{100-y}V_y$ alloys using neutron diffraction

[1]BS Jacobs, [1]ARE Prinsloo, [1]CJ Sheppard, [2]AM Venter and [3]HE Maynard-Casely

[1]Department of Physics, University of Johannesburg, PO Box 524, Auckland Park, 2006, South Africa
[2]Research and Development Division, NECSA limited, P. O. Box 582, Pretoria 0001, South Africa
[3]Bragg Institute, ANSTO, Locked Bag 2001, Kirrawee DC NSW 2232, Australia

E-mail address: sjacobs@uj.ac.za

Abstract. This paper reports preliminary results of neutron diffraction investigations of the $(Cr_{84}Re_{16})_{100-y}V_y$ alloy system, with y = 0, 4.2 and 6.2. The previously reported magnetic phase diagram for this alloy system compiled from various physical property studies indicates a possible critical concentration existing at $y_c \approx 10.5$. Amongst others, anomalies were observed in graphs of the Sommerfeld coefficient (γ) as function of y, close to the critical concentration, as well as at $y \approx 4$. The latter warranted further investigation using neutron diffraction in order to shed light on the conjecture that the minima corresponds to the existence of an incommensurate (I) spin-density-wave (SDW) to commensurate (C) SDW transition.

1. Introduction

Neutron diffraction has become indispensable in the investigation of the magnetic structure of elements and alloys. This technique was specifically used by Shull and Wilkinson to elucidate the antiferromagnetic (AFM) structure of pure Cr [1]. Cr and its dilute alloys display magnetic ordering characterized by a spin-density-wave (SDW) that is established thorough Coulombic interactions between the hole and electron sheets at the Fermi surface, a mechanism referred to as nesting [2]. This nesting decreases the energy of the system through electron-hole pair condensation and results in the appearance of SDW energy gaps at the Fermi surface in specific k-space directions when cooled through the Néel temperature (T_N). The nesting area, and concomitantly the stability of the SDW state, depends on the electron concentration per atom (e/a) which can easily be tuned by alloying Cr (e/a = 6) with elements like V (e/a = 5) or Mn (e/a = 7) to respectively decrease or increase the electron concentration. In pure Cr, the electron sheet is slightly smaller than the hole sheet, resulting in a SDW that is incommensurate (I) with the lattice [2]. Alloying Cr with Re, an electron donor having e/a = 7, brings the size of the electron and hole Fermi sheets more in line with each other. The SDW eventually becomes commensurate (C) with the lattice at a Re concentration of about 0.3 at.%. The concentration (c) versus temperature (T) magnetic phase diagram of the $Cr_{100-c}Re_c$ alloy system thus exhibits three AFM SDW phases – the longitudinal (L) ISDW, the transverse (T) ISDW and the CSDW with a triple point at $c_t \approx 0.3$ at.% Re where the ISDW, CSDW and paramagnetic (P) phases coexist [2].

Possible quantum critical behaviour (QCB) in the $(Cr_{84}Re_{16})_{100-y}V_y$ alloy system has been reported [3]. One of the significant indicators of QCB in Cr alloy systems is the behaviour of the Sommerfeld coefficient, γ [4,5] that is obtained by fitting the low temperature specific heat (C_p) data to the equation

$C_p = \gamma T + \beta T^3$. A broad deep minimum was observed in the $\gamma(y)$ curve of the $(Cr_{84}Re_{16})_{100-y}V_y$ alloy series at $y \approx 4$, after which it increased continuously on increasing y reaching a maximum at $y \approx 9$. This was followed by a continuous decrease through the critical concentration $y_c \approx 10.5$ and levelling off in the paramagnetic (PM) phase. The decrease in γ through the critical concentration can be attributed to changes in the density of states at the Fermi surface [4]. It was proposed that the minima observed at $y \approx 4$ could correspond to a CSDW-ISDW transition. Neutron diffraction studies were performed to establish this. This study reports on preliminary neutron diffraction investigations into the magnetic phases that exist in the $(Cr_{84}Re_{16})_{100-y}V_y$ alloy system as function of temperature.

2. Experimental

Ternary $(Cr_{84}Re_{16})_{100-y}V_y$ alloys with y = 0, 4.2 and 6.2 were prepared by arc melting in a purified argon atmosphere from Cr, Re and V each having mass fractional purities 99.99 %, 99.99 % and 99.8 % respectively. Special emphasis was placed on synthesizing specimens with high homogeneity and metallurgical quality. The alloys were annealed in an ultra-high purity argon atmosphere at 1343 K for seven days and quenched into iced water. The elemental composition and homogeneity were determined using electron microprobe analyses. Electrical resistance (R) was measured over 2 K $\leq T \leq$ 390 K, using a standard Physical Properties Measurement System (PPMS) [6]. Resistance measurements at temperatures above 390 K were performed using resistive heating in an inert atmosphere using the standard dc four-probe method and current reversal with Keithley instrumentation. Magnetic susceptibility (χ) was measured over 2 K $\leq T \leq$ 390 K using a SQUID-type magnetometer based on the Magnetic Properties Measurement System (MPMS) platform of Quantum Design [6]. The samples were cooled to 2 K in zero field and the susceptibility measurements subsequently done upon heating in a field of 100 Oe. For the neutron powder diffraction investigations, the alloys were pulverised after annealing to limit the presence of large grains and render more uniform intensity distributions over the Debye Scherer cones. Neutron diffraction measurements were performed over the temperature range 10 K $\leq T \leq$ 350 K on the Wombat powder diffractometer [7] at the Australian Nuclear Science and Technology Organisation (ANSTO) using a wavelength of 0.241 nm and with the primary beam filtered with a pyrolytic graphite filter to reduce higher order wavelength contaminations.

3. Results and discussion

Figure 1(a) shows the X-ray diffraction (XRD) pattern for the $(Cr_{84}Re_{16})_{95.8}V_{4.2}$ sample that was taken with Cu radiation (0.154nm wavelength). Since V neighbours Cr in the periodic table with atomic mass and size close to that of pure Cr, its addition produces the least perturbation on the structure of pure Cr [2]. The diffraction pattern of the $(Cr_{84}Re_{16})_{95.8}V_{4.2}$ sample is well fitted to the XRD pattern of

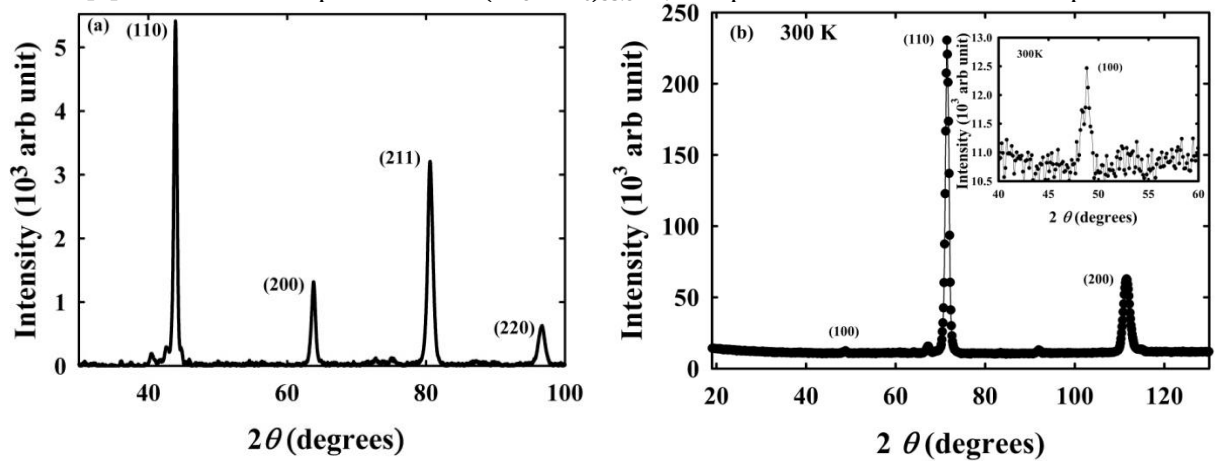

Figure 1: (a) The XRD pattern for the $(Cr_{84}Re_{16})_{95.8}V_{4.2}$ sample with the Bragg peaks indexed and (b) the neutron diffraction pattern for the $(Cr_{84}Re_{16})_{95.8}V_{4.2}$ sample at 300 K with (100) peak in inset.

body centred cubic (bcc) Cr by adjusting the lattice parameter to 0.29210 nm for this alloy from the value of 0.28839 nm for pure Cr. Peak to the left of the (110) peak corresponds to an oxide of Cr. Even though much care is taken during the melting process, the presence of small amounts of oxide is inevitable. Figure 1(b) shows the neutron diffraction pattern for the $(Cr_{84}Re_{16})_{95.8}V_{4.2}$ sample at 300 K with the (100) peak shown in the inset.

The $R(T)$ curves for $Cr_{84}Re_{16}$ and $(Cr_{84}Re_{16})_{100-y}V_y$, with y = 4.2 and 6.2, are shown in figure 2. Temperature of the minimum in $dR(T)/dT$ accompanying the $R(T)$ magnetic anomaly is defined as T_N [2]. In general, the size of the anomaly, as well as T_N, decreases with increase in V concentration. The anomalies, which appear as a sudden increase in resistance on cooling through T_N, can be attributed to the Coulombic interactions of electron and hole Fermi surfaces from the nesting process on SDW formation [2].

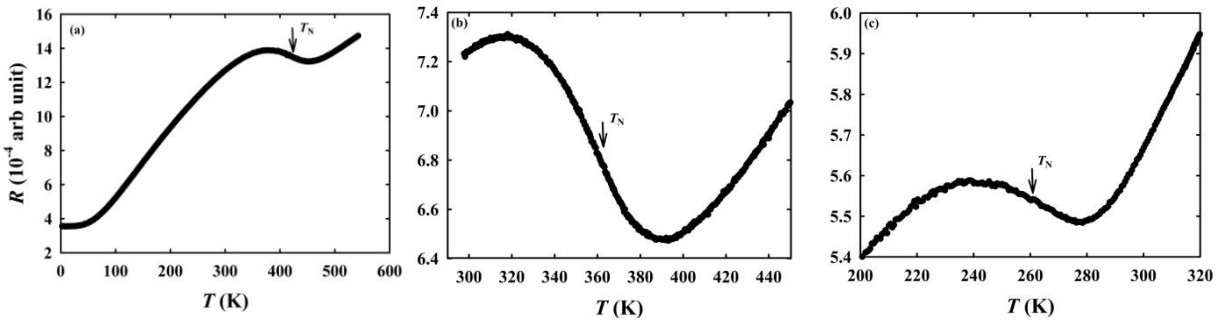

Figure 2: The $R(T)$ curves for the $(Cr_{84}Re_{16})_{100-y}V_y$ alloy system with, with (a) y = 0, (b) y = 4.2 and (c) y = 6.2. Arrow indicates the position of T_N for each alloy.

The temperature dependence of normalized susceptibility for $(Cr_{84}Re_{16})_{95.8}V_{4.2}$ is shown in figure 3 as an example of the typical trends of the samples. Compared with results from other previous studies [8, 9], broad anomalies are seen in the χ-T curves of all the samples of this study. The Néel transition temperature is taken at the point where a kink in the temperature dependence of χ occurs on cooling from the paramagnetic to antiferromagnetic phase. The decrease in χ can be attributed to the decrease in the density of states at the Fermi energy due to the SDW energy gap formation [2]. The broken line in figure 3 serves as a guide to the eye indicating the trend of the curve, should the sample have remained paramagnetic. T_N is taken at the point where the measured values deviate from the broken

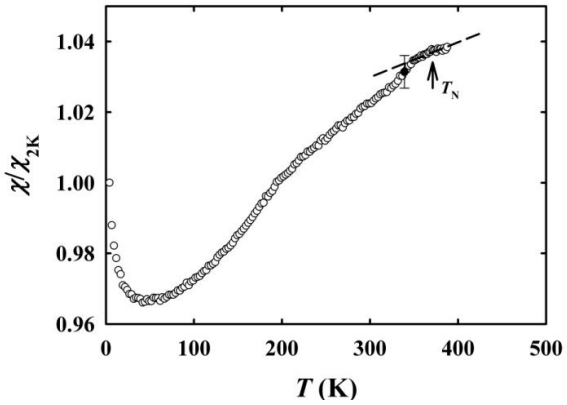

Figure 3. The temperature dependence of normalized susceptibility for the $(Cr_{84}Re_{16})_{95.8}V_{4.2}$ alloy.

line and the T_N obtained in this manner corresponds well with T_N obtained from reported electrical resistivity and thermal transport measurements [3]. The low temperature upturn in the curves is ascribed to the effect of a Curie tail that may arise from the presence of oxide impurities [10].

The neutron diffraction patterns of $Cr_{84}Re_{16}$ and $(Cr_{84}Re_{16})_{95.8}V_{4.2}$ alloys are shown in figure 4. Figure 5 shows the diffraction patterns for the $(Cr_{84}Re_{16})_{93.8}V_{6.2}$ alloy. Pure Cr has a magnetic moment of 0.4 μ_B and due to its antiferromagnetic structure, the magnetic moments manifest at the (100) lattice parameter position [11]. The commensurate phase is characterised by the moments located at the corners of the unit cell being parallel to each other but antiparallel to the one at the centre [12]. For the CSDW phase the unit cell lengths of the chemical and magnetic structures are the same. As the moments are collinear to the equivalent {100} planes, the resulting neutron diffraction pattern will have magnetic Bragg peaks at {100}, {111}, {210}, etc. Since the magnetic moment of Cr is weak, only the {100} magnetic peak is observed [12]. The ISDW phase leads to the additional presence of magnetic satellites, offset from the {100} positions at (1±δ,0,0) reciprocal lattice positions [13], whereas the CSDW phase displays no such satellites.

Figure 4(a) shows the neutron diffraction pattern for the $Cr_{84}Re_{16}$ mother alloy taken at 300 K and at the highest measured temperature, 560 K (expected T_N = 420 K). A clear temperature dependent peak of magnetic origin that dies out is seen at 2θ = 48.7° which corresponds to the (100) position. The second peak at 2θ = 38° is not strongly dependent on temperature and therefore is not magnetic in origin. Within the detection limit of the instrument, since no satellite peaks of magnetic origin are observed, it is concluded that this alloy has a CSDW ordering at room temperature, in correspondence to what is expected from the Cr-Re magnetic phase diagram [2].

The neutron diffraction patterns for the $(Cr_{84}Re_{16})_{95.8}V_{4.2}$ alloy taken at various temperatures are shown in figure 4(b). T_N for this alloy is 370 K. Due to time constraint, a reference paramagnetic diffraction pattern was not recorded. Measurements started at 340 K where a central magnetic peak could be observed at the (100) position. On cooling to 300 K, the (100) intensity grows and in addition a peak appears at approximately 2θ = 38.6° that corresponds to the (1+δ,0,0) magnetic satellite. On

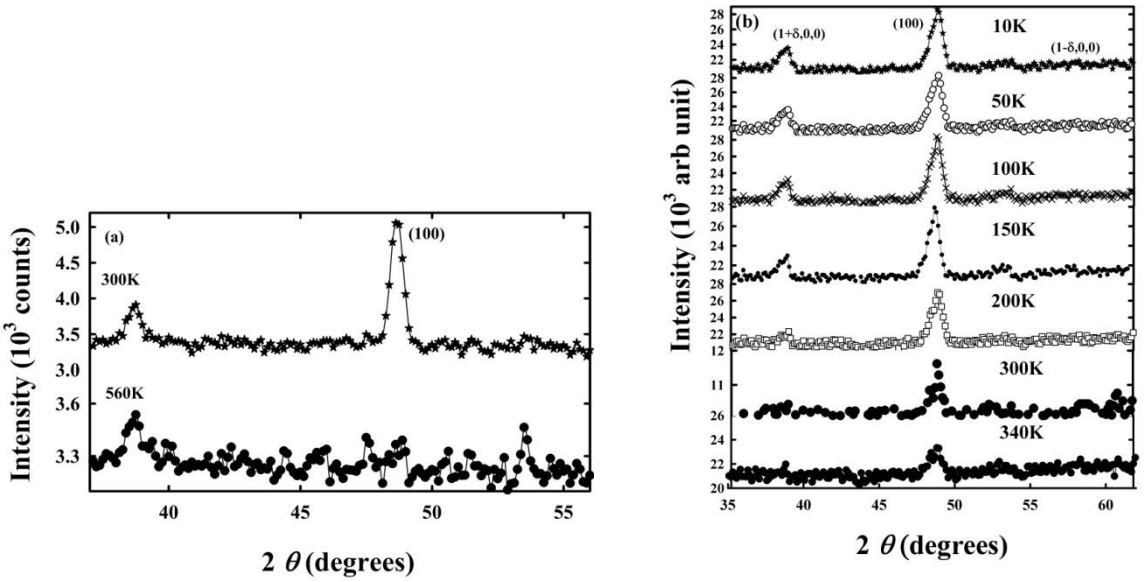

Figure 4. Neutron diffraction patterns of $(Cr_{84}Re_{16})_{100-y}V_y$ alloys, with (a) y = 0 at 300 K and 560 K and (b) y = 4.2 at various temperatures.

further cooling, the intensities of both of these magnetic peaks increase. The calculated full width at half maximum (FWHM) shows no regular trend. The (1-δ,0,0) magnetic satellite is expected at the $2\theta = 58.8°$ position but was not observed. Although the satellite peak on the right is observed at certain temperatures, no clear trend is exhibited. These results indicate that the $(Cr_{84}Re_{16})_{95.8}V_{4.2}$ alloy appears to undergo a transition from the CSDW phase at $T > 300$ K to a certain ISDW phase at $T \leq 300$ K, as proposed initially [3].

Figure 5 shows the diffraction pattern for the $(Cr_{84}Re_{16})_{93.8}V_{6.2}$ alloy at various temperatures. T_N for this alloy is 270 K. The diffraction pattern observed at 300 K corresponds to the paramagnetic phase. At 220 K, the central (100) peak is observed indicating the CSDW phase and it appears to remain in the CSDW phase up to 180 K. However, longer measurement times will be required to confirm this. Below 180 K, the existence of a satellite reflection can be detected.

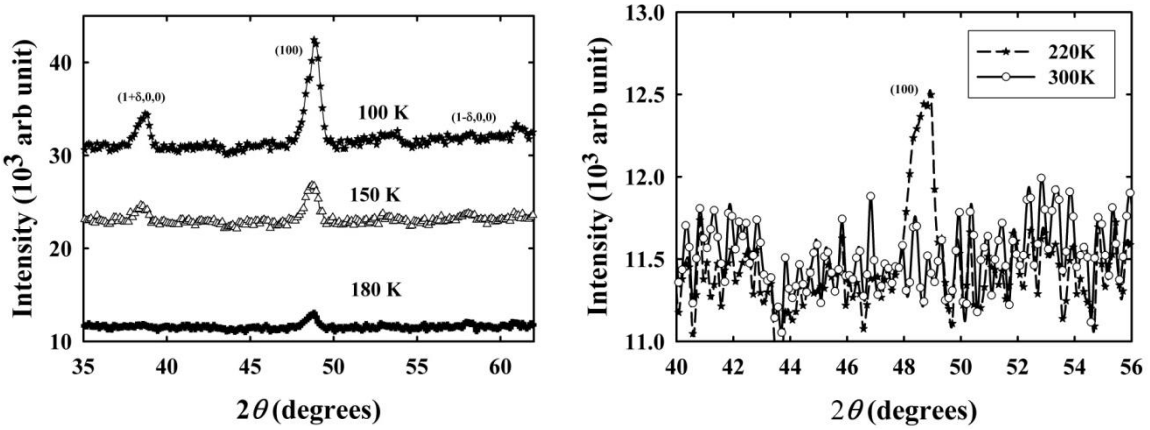

Figure 5. The neutron diffraction patterns of the $(Cr_{84}Re_{16})_{93.8}V_{6.2}$ alloy. The alloy remains in the ISDW phase up to 180 K. At 220 K, the absence of symmetrical satellite peaks indicate CSDW ordering.

The increase in intensity of the central peak and the satellite peak at temperatures below 180 K indicates that the alloy is in the ISDW phase. A symmetric satellite peak on the right hand side is also observed though not very distinct and the variation in its intensity with temperature is not as prominent as the satellite peak on the left. The $(Cr_{84}Re_{16})_{93.8}V_{6.2}$ alloy thus appears to be in the CSDW phase at $T \geq 180$ K, transforming to a ISDW phase at $T < 180$ K.

4. Conclusion.

The present study investigated the possible magnetic origin of the broad minimum observed in the $\gamma(y)$ curve of the $(Cr_{84}Re_{16})_{100-y}V_y$ alloy series at $y \approx 4$. The limited beam time awarded on the Wombat diffractometer at ANSTO was utilised to only probe the magnetic phases of the $Cr_{84}Re_{16}$, $(Cr_{84}Re_{16})_{95.8}V_{4.2}$ and $(Cr_{84}Re_{16})_{93.8}V_{6.2}$ alloys. At room temperature, the $Cr_{84}Re_{16}$ alloy is in the CSDW phase. Measurements need to be extended to a wider temperature range to further investigate the magnetic ordering in this sample. Preliminary measurements on the $(Cr_{84}Re_{16})_{95.8}V_{4.2}$ alloy indicate satellites around the central (100) peak in the neutron diffraction pattern suggesting that this alloy is in the ISDW phase at $T \leq 300$ K. In the case of the $(Cr_{84}Re_{16})_{93.8}V_{6.2}$ alloy, diffraction patterns indicate the ISDW phase at $T < 180$ K. At the first glance, these preliminary results seem to concur with our initial projection that the minimum in the $\gamma(y)$ curve corresponds to an I-C transition of the SDW state. Measurements need to be extended for the $(Cr_{84}Re_{16})_{100-y}V_y$ series to include temperatures scans for the $y = 0$ sample and higher temperatures for the $y = 4.2$ sample. It is also essential to repeat the preliminary measurements with improved counting statistics. Neutron diffraction study also needs to be extended to include samples having V concentration between 4.2 and 6.2 in order to make concrete conclusions.

Acknowledgements
This work was supported by the NRF of South Africa under Grants 80626, 80928 and the Faculty of Science at the University of Johannesburg.

References
[1] Shull C G and Wilkinson M K 1955 *Phys. Rev.* **97** 304
[2] Fawcett E, Alberts H L, Galkin V Y, Noakes D R and Yakhmi J V 1994 *Rev. Mod. Phys.* **66** 25
[3] Jacobs B S, Prinsloo A R E, Sheppard C J and Strydom A M 2013 *J. Appl. Phys.* **113** 17E126
[4] Takeuchi J, Sasakura H and Masuda Y 1980 *J. Phys. Soc. Japan* **49** 508
[5] Yeh A, Soh Y, Brooke J, Aeppli G and Rosenbaum TF 2002 *Nature* **419** 459
[6] Quantum Design Inc, 6325 Lusk Boulevard, San Diego, USA
[7] Studer A J, Hagen M E and Noakes T J 2006 *Physica B* **385-386** 1013
[8] Nishihara Y, Yamaguchi Y, Waki S and Kohara T 1983 *J. Phys. Soc. Japan* **52**(7) 2301
[9] Arajs A, Kote G, Moyer CA, Kelly JR, Rao KV and Anderson EE 1976 *Phys. Stat. Sol. (b)* **74** K23
[10] Wagner M J, Dye J L, Pérez-Condero E, Bulgas R and Echegoyen L 1995 *J. Am. Chem. Soc.* **117** 1318
[11] Bacon G E and Cowlam N, 1969 J. Phys. **C2** 238
[12] Papoular R, Debray D and Arajs S 1981 *J. Magn. Magn. Mater.***24** 106-110
[13] Bacon G E 1961 *Acta. Cryst.* **14** 823